

Article

The Effect of Water Injection on the Control of In-Cylinder Pressure and Enhanced Power Output in a Four-Stroke Spark-Ignition Engine

Mingrui Wei ^{1,2}, Thanh Sa Nguyen ^{1,2,3,*}, Richard Fiifi Turkson ^{1,2,4}, Guanlun Guo ^{1,2} and Jinping Liu ^{1,2}

¹ Hubei Key Laboratory of Advanced Technology for Automotive Components, Wuhan University of Technology, Wuhan 430070, China; weimingrui@whut.edu.cn (M.W.); rrturkson@hopoly.edu.gh (R.F.T.); glguo@whut.edu.cn (G.G.); liujinpinglucky@163.com (J.L.)

² Hubei Collaborative Innovation Center for Automotive Components Technology, Wuhan University of Technology, Wuhan 430070, China

³ Faculty of Mechanical Engineering, HoChiMinh University of Transport, HoChiMinh City 760000, Vietnam

⁴ Mechanical Engineering Department, Ho Polytechnic, P.O. Box HP 217, Ho 036, Ghana

* Correspondence: nguyenthansa@gmail.com; Tel.: +84-906-332-284

Academic Editor: Marc A. Rosen

Received: 14 June 2016; Accepted: 24 September 2016; Published: 30 September 2016

Abstract: This paper presents the results for liquid water injection (WI) into a cylinder during the compression and expansion strokes of an internal combustion engine (ICE), with the aim of achieving an optimal in-cylinder pressure and improving power output using CFD simulation. Employing WI during the compression stroke at 80° of crank angle (CA) before top dead centre (bTDC) resulted in the reduction of compression work due to a reduction in peak compression pressure by a margin of about 2%. The decreased peak compression pressure also yielded the benefit of a decrease in NO_x emission by a margin of 34% as well as the prevention of detonation. Using WI during the expansion stroke (after top dead centre–aTDC) revealed two stages of the in-cylinder pressure: the first stage involved a decrease in pressure by heat absorption, and the second stage involved an increase in the pressure as a result of an increase in the steam volume via expansion. For the case of water addition (WA 3.0%) and a water temperature of 100 °C, the percentage decrease of in-cylinder pressure was 2.7% during the first stage and a 2.5% pressure increase during the second stage. Water injection helped in reducing the energy losses resulting from the transfer of heat to the walls and exhaust gases. At 180° CA aTDC, the exhaust gas temperature decreased by 42 K, 89 K, and 136 K for WA 1.0, WA 2.0, and WA 3.0, respectively. Increasing the WI temperature to 200 °C resulted in a decrease of the in-cylinder pressure by 1.0% during the first stage, with an increase of approximately 4.0% in the second stage. The use of WI in both compression and expansion strokes resulted in a maximum increase of in-cylinder pressure of about 7%, demonstrating the potential of higher power output.

Keywords: CFD simulation; engine efficiency; heat losses; heat transfer; water addition; water injection

1. Introduction

In recent years, concerns over environmental pollution and energy balance has resulted in major interest in research regarding the optimal design of internal combustion engines (ICEs), especially automobile engines. There is an increasing trend of the quantity of automobiles sold (including passenger and commercial vehicles) in the world on a year-to-year basis. With the increase in the number of vehicles produced each year, it is accompanied with an increase in the number of engines produced because ICEs currently represent the prime source of power for automobiles. Thus,

improving the efficiency of ICEs using different methods leads to considerable benefits accruing from the production of more engine power while utilizing less fuel than would normally be the case.

The utilization of liquid WI in spark-ignition (SI) engines has been studied for a number of years by many researchers to reduce NO_x emissions [1,2]. In one study [3], hydroxide and hydrogen were formed from the thermal-dissociation process of water at high temperature, which absorbed the heat during combustion. Hence, this method is useful for controlling the peak in-cylinder temperature and for reducing unwanted emissions. Nande et al. [1] concluded that WI is an improved technique for reducing NO_x emissions based on an investigation conducted on a hydrogen-fueled SI engine combined with in-cylinder direct WI. In another study, water was injected into the intake manifold to investigate the effects of water on anti-knock ability and the possible reduction in compression work [4]. The study concluded that this WI technology has benefits for anti-knock and higher power output by reducing the work done during the compression stroke. Water was injected into the inlet port up to four times the amount of fuel injected to estimate the effects on combustion and pollutant emission [5].

Many different ratios of water to fuel mass were applied for injecting water into ICEs. Karagöz et al. [6] investigated the addition of hydro-oxygen and water to the intake system of an SI engine using up to 25% of water mass relative to gasoline mass for studying the performance of the engine and emission levels. Using a single cylinder engine, Feng et al. [7] experimented with two kinds of fuel; pure gasoline and 35% volume butanol–gasoline blend +1% H₂O addition in different operating modes. The results demonstrated that engine performance, brake specific fuel consumption (BSFC), and CO and HC emissions of the fuel blends were better than those of pure gasoline for the test conditions considered. For a small SI engine driving a generator, Munsin [8] investigated the effects of hydrous ethanol with high water contents up to 40%. Injected water had the effect of reducing NO_x emissions by a margin of up to approximately 35% in comparison with pure gasoline. WI technology was also evaluated as an effective method for controlling emission levels and for achieving an enhanced engine performance [5].

The effect of WI on engine performance was also explored in the study conducted by Sari et al. [9] with high water content ethanol mixtures from 5%–40% of mass in 0.668 L of a single-cylinder port injected SI engine. An increased water content enhanced knock avoidance capabilities and aqueous alcohol injection showed promise for higher engine efficiency and lower fuel costs. The conclusion of the study also pointed to the fact that as the WI level supplied to the engine increased, the percentage of useful work increased, while the losses other than unaccounted losses decreased [3]. Based on CFD results, Boretti et al. [10] showed that the brake thermal efficiency was improved by more than 55% with 200% of injected water by mass in comparison with the mass of oxygen and hydrogen mixture operating with a significant amount of exhaust gas recirculation.

WI in an ICE is not only useful for enhancing anti-knock capabilities and emission reduction but also yields benefits in the recycling of waste energy from the exhaust gas. The cylinder of an ICE has a limitation in the expansion ratio; that is the burnt air-fuel mixture cannot fully expand in the cylinder. Because the temperature and pressure of exhaust gas are higher than that of ambient conditions, the engine exhaust gas contains pressure energy and thermal energy [11]. Since only about 12%–25% of fuel energy will be used to drive the wheels, some of the thermal energy escapes from engine through the exhaust gases, while the remainder of the energy balance is accounted for by friction, coolant, and other means [12–16]. Based on the heat balance in ICEs (including diesel and gasoline), Wang et al. [17] and Dolz et al. [18] proffered that only about one third of a fuel's chemical energy is converted into useful work and that the remainder of the energy is lost to the operating environment. According to the research conducted by Wang et al. [19], the temperature of the exhaust gas was around 800 K while in another study, a 600–700 K exhaust temperature was reported [20]. In recycling the exhaust gas energy of ICEs, the thermal efficiency is improved leading to significant improvements in power output, fuel economy, and emission levels.

Moreover, in the work of Hatazawa et al. [21], Stabler [12], Taylor [13], Yu and Chau [22], and Yang [23], it was stated that 30%–40% of waste heat produced from the fuel burning process was lost to the environment through the exhaust gases. Thus, fuel energy cannot be completely converted into useful work and a significant amount of energy is lost through the transfer of heat to the cylinder walls and to the exhaust gases. If only 6% of the heat contained in exhaust gases is converted into electrical power, this would mean a reduction of fuel consumption by 10% due to the decrease in mechanical losses [24]. Other studies stated that an increase of 20% in fuel efficiency can be easily achieved by converting about 10% of the waste heat into useful work [23,25].

Using WI in combination with the Rankine cycle or Organic Rankine cycle to improve ICE energy efficiency is one method of engine exhaust gas energy recovery. The exhaust pipe is coupled with a Rankine steam cycle system and the high temperature exhaust gas is used to generate steam [26]. This study involved the coupling of a traditional ICE cycle with the steam expansion cycle using steam injection into the expanding cylinder. In this way, the engine thermal efficiency can be improved by 6.3% at 6000 r/min. Based on experimental work by Endo et al. [27], the thermal recovery system showed a maximum thermal cycle efficiency of 13%. In a similar study conducted by Bari and Hossain [28], an additional increase in power of 16% was realized. After system optimization, the additional power increased from 16% to 23.7%. The waste heat from the exhaust gases and cooling water was used in a Homogeneous Charge Compression Ignition (HCCI) engine in the work of Sarabchi [29]. The theoretical thermal efficiency of the system was 5.19% higher than that of the HCCI engine, while the reduction in CO₂ emission was 4.067%. The wasted heat recovery technology was also applied on a hydrogen-fueled internal combustion engine (HICE) because more heat is wasted by the HICE, and it produces nearly three times more water than a conventional engine [30]. A waste heat recovery sub-system was used to improve the overall thermal efficiency from 27.2% to 33.6% at engine speeds starting from 1500 to 4500 rpm.

In another study [31], water was injected directly into the cylinder to enhance the efficiency of the engine in recovering the wasted heat. Using the waste heat from the exhaust gas and engine coolant system to heat up the injected water, the theoretical thermal efficiency of the ICE reached 53% and 67% when the WI temperature was 120 °C and 200 °C, respectively.

From the reviews on WI in ICEs, WI has a good effect in reducing emissions, especially NO emissions. Injected water has been used as an absorbent for waste heat recovery. However, injected water can affect engine power output during the decrease or increase of in-cylinder pressure which takes place when the injected water absorbs heat and evaporates, respectively. In this study, the injection of liquid water into the intake system of a four-stroke engine equipped with a gasoline direct injection (GDI) system was considered for enhancing the in-cylinder pressure by the use of the AVL Fire CFD simulation code. Water was injected during the compression stroke to control compression pressure and thus reduce compression work. On the other hand, water was injected in the expansion stroke to improve the expansion pressure by taking advantage of the volumetric expansion of steam. The benefits of WI in the ICE were significant by the timed injection of water during the compression and expansion strokes. The effects of WI (for simulation cases) on in-cylinder pressure, heat transfer, NO emission, and other factors were examined and are discussed in this study.

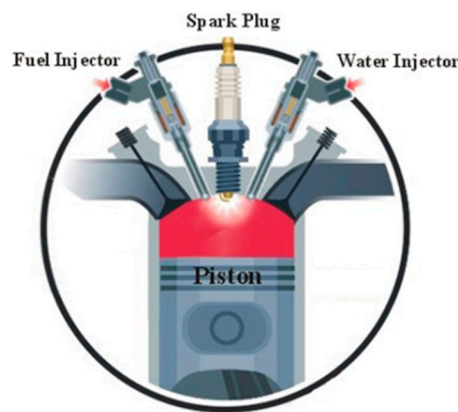
2. Studied Model

A GDI engine model with an axisymmetric cylinder was used for the current study, the parameters of which are presented in Table 1.

Two injectors were used in the studied engine model: one for controlling fuel injection and the other for water injection, as illustrated in Figure 1. An engine model was used with gasoline as a primary reference fuel (fuel comprised of 10% n-heptane and 90% iso-octane). Fuel was injected at a rate of 2.332×10^{-5} kg/cycle and the fuel temperature was fixed at 20 °C. The water injector was installed adjacent to the spark plug on the single cylinder engine.

Table 1. Engine parameters.

Description	Details
ICE type	Single-cylinder GDI
Compression ratio	13
Bore [mm]	80
Stroke [mm]	81.4
Displacement [cm ³]	441
Engine speed [rpm]	2000
Ignition timing	20° CA bTDC
Fuel injection timing	60° CA bTDC
Fuel injection duration [° CA]	20

**Figure 1.** Schematic illustration of the injector position in the numerical investigation.

As previously stated, this paper used AVL-Fire for performing CFD simulation of the liquid water injection into the engine cylinder in an attempt to improve the in-cylinder pressure. The 3D geometrical shapes of the ICE were built using the Pro-Engineer software (Parametric Technology Corporation, Needham, MA, US). The computational domain was divided into three regions: the manifold intake region, the exhaust pipe region, and the piston-chamber region. It was necessary for the piston and valves to move according to the resolution of the crank angle and thus, the Fame Engine Plus module was used for generating the moving mesh. Figure 2 presents the engine model in the simulation domain.

**Figure 2.** The engine model used for the simulation.

Fame Engine Plus was employed for producing 3D hexahedral cells for the engine moving mesh, and involved the intake port and valves, the cylinder head, the combustion chamber, and the exhaust port and valves. The hexahedral cells were employed for mesh generation due to the better accuracy and stability compared to the tetrahedral cells [32]. The number of cells was about 168,498 at top dead centre (TDC) position and around 436,286 cells at bottom dead centre (BDC) position; about half of the cells of the computational mesh around the valves and combustion chamber were concentrated to obtain accurate results. The type and size of simulation mesh have an effect on the simulation

results and calculation time. In this study, the concept of mesh was chosen in the comparison of about 43,398 cells at the TDC position and approximately 163,110 cells at the BDC position [32] in a similar simulation of an engine model. The number of cells was also compared with 90,000 cells at TDC and approximately 180,000–200,000 cells at BDC in a study regarding the combustion process in a compressed natural gas direct injection engine with both simulation and experimental studies [33]. Figure 3 illustrates the numerical mesh of the engine model with the piston at the TDC position.

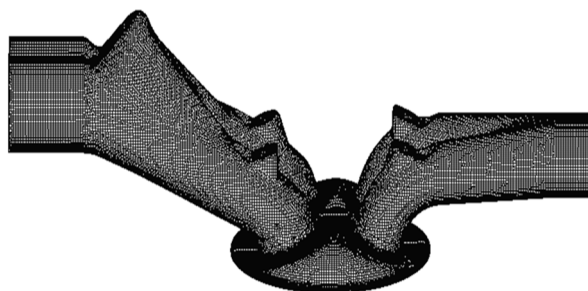


Figure 3. Numerical mesh for the piston position at TDC.

The equations governing the dynamics of gases were the expressions for conservation and the thermodynamic laws. Gases were defined as being compressible viscous fluids. The equations governing the in-flow model included the mass conservation equation, momentum conservation, and the energy conservation equation. The standard model $k-\varepsilon$ was used for solving the in-cylinder flow problems. The turbulence model employed was the $k-\varepsilon$ turbulence model for compressible fluids and high Reynolds number flow [34], where k is the turbulence kinetic energy and ε is the turbulence dissipation rate. The SIMPLE algorithm was employed to solve the resulting algebraic equations, based on the pressure-correction method. The pressure-corrections were used to update the pressure and velocity fields so that the velocity components obtained from the solution of the momentum equations satisfied the continuity equation. A second order discretization scheme was used for the momentum equations, turbulent kinetic energy, and dissipation rate in combination with the $k-\varepsilon$ turbulence model.

One complete engine cycle was simulated at 360° CA bTDC at the beginning of the intake stroke to 360° CA aTDC at the end of the exhaust stroke with a calculus step of 1.0° CA. For the boundary conditions, an inlet mass was applied at the entry surface of the manifold and a pressure outlet was imposed at the exit surface of the exhaust duct. The rest of the geometry was considered as an impenetrable wall and the temperatures were suitably set as given in Table 2. In the simulation, intake air was assumed to be an ideal gas and inlet mass flow rate was also assumed as a constant [33]. Its density will therefore be variable. However, the viscosity, thermal conductivity, and specific heat capacity at constant pressure remained constant.

Table 2. Boundary conditions.

Boundary Condition	Value
Inlet mass flow rate [g/s]	0.5
Outlet pressure [bar]	1.3
Manifold wall [K]	330
Exhaust wall [K]	550
Piston [K]	450
Intake valve [K]	330
Exhaust valve [K]	550
Chamber [K]	450
Cylinder [K]	450

The initial temperature and pressure in the engine cylinder needed to be established to provide the initial conditions for solving governing equations. The initial pressure at 360° CA bTDC was fixed

at 1.15 bar. An initial temperature of 900 K was set for the residual exhaust gas at the beginning of the intake stroke. The value of the turbulent kinetic energy k was assumed to be spatially uniform and was set to 5% of the kinetic energy of the mean piston speed.

For the combustion model, the Eddy Break-up Model was used; and for NO formation, the Original Heywood Model. The Eddy Break-up model was used as the combustion model because it was considered as a typical example of the mixed-is-burnt combustion model. This combustion model assumes that the chemical reactions are completed at the moment of mixing, so that turbulent mixing completely controls the reaction rate. A multi-component model was employed as the evaporation model and Tab model for the break-up model. For the effect of wall interaction, the Walljet0 was applied.

3. Results and Discussion

3.1. Water Addition During the Compression Stroke

In this section, water was directly injected into the cylinder during the compression stroke in order to examine the effects of injected water on the in-cylinder pressure and average surface temperature of the cylinder walls from the heat transfer process. The WI during this period also had an effect on the combustion process and emissions. The parameters of WI and water addition (WA) mass are presented in Table 3.

Table 3. Parameters of WI.

Parameter	Value
Injection Timing	80° CA bTDC
Water duration [° CA]	10
Water temperature [K]	310
Water mass [Kg]	5% (WA 5); 10% (WA 10); 15% (WA 15); 20% (WA 20); 25% (WA 25) in relation to fuel mass

3.1.1. Effects on the In-Cylinder Pressure

After the direct injection of water into the cylinder, the liquid water absorbed the heat of the compressed gas. During the first stage, injected water results in the cooling of the compressed charge. The temperature change under the effect of WI is indicated in Figure 4. The compressed gas temperature was decreased, leading to the decrease of the in-cylinder pressure. Figure 5 illustrates the decrease of the in-cylinder pressure during the latter stages of the compression stroke.

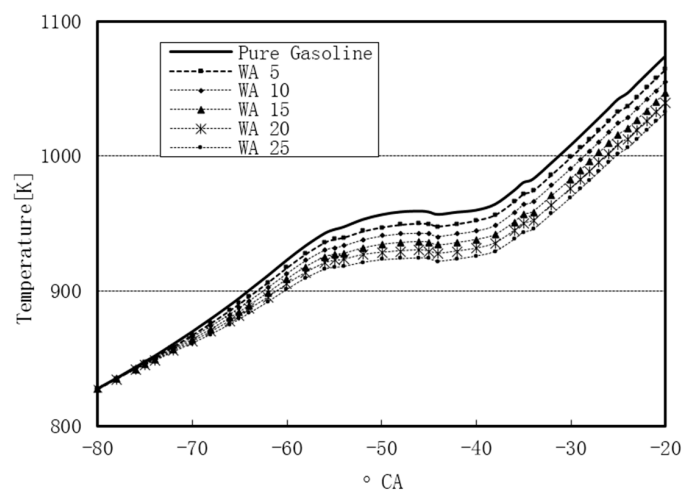


Figure 4. The decrease in compressed charge temperature as a consequence of injected water.

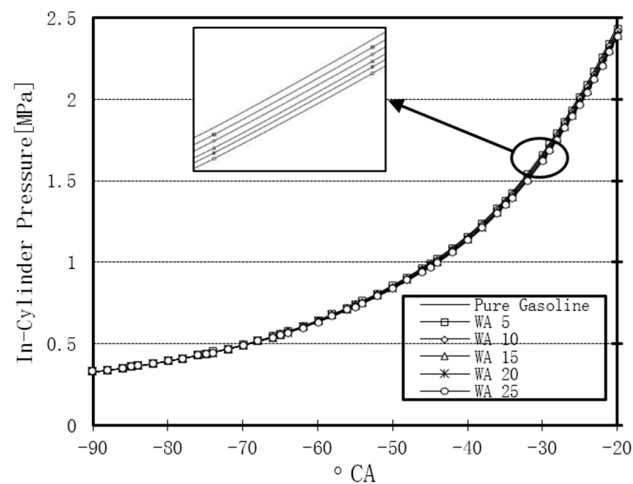


Figure 5. The decrease of in-cylinder pressure during the latter stages of the compression stroke.

As illustrated in Figure 5, there is a slight decrease of in-cylinder pressure in comparison with the pure gasoline case. Thus, the use of WI during the compression stroke had the effect of reducing the compression work. The reduction of compression work is one of the techniques for improving engine power. Particularly, the reduction of compression work has a considerable significance for high compression ratio engines because of the high compression pressure at the later stages of the compression stroke.

After 20° CA bTDC, the combustion was initiated by the introduction of a spark into the combustion chamber. The in-cylinder fluid temperature increased quickly, with the injected water heated to the point where an overheated steam was formed. The volumetric expansion of steam took place during the combustion period. Figure 6 illustrates the increase in the peak in-cylinder pressure for the volumetric expansion of steam.

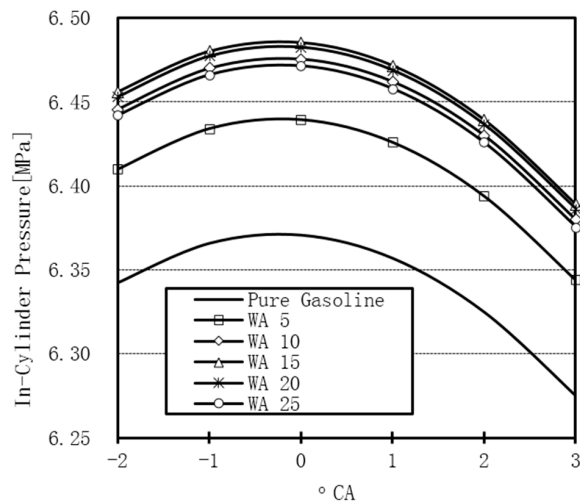


Figure 6. The increase of peak in-cylinder pressure for the volumetric expansion of steam.

As can be seen in Figure 6, 25% of the WI mass in comparison with the fuel mass did not yield the highest pressure because of excessive heat absorption during the compression stroke. Fifteen percent (15%) of the WI mass yielded the highest peak-pressure, representing about 2% increase in the peak in-cylinder pressure.

With the availability of WI mass, it is possible to realize an increase of in-cylinder pressure during the combustion-expansion process and thus facilitate the achievement of a higher power output,

as shown in Figure 7. It follows, therefore, that the use of WI leads to an improvement in the power output without the use of extra fuel.

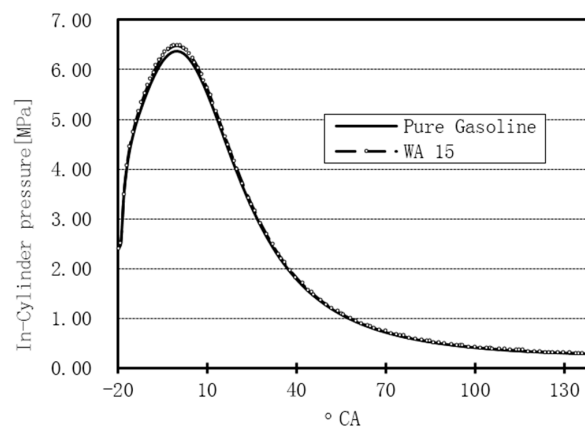


Figure 7. The in-cylinder pressure during the combustion-expansion process with the use of 15% WI in comparison with the pure gasoline case.

3.1.2. Effects of WI on the Reduction in Energy Losses via Heat Transfer

During engine operation, there are energy losses via heat transfer to the cylinder walls during the latter stages of the compression stroke and the combustion-expansion stroke. During the compression process, the charge temperature rises above the wall temperature and thus heat transfer occurs from the in-cylinder gasses to the cylinder walls. In the combustion-expansion stroke, the heat transfer rate to the cylinder walls is the highest. Among the energy loss through heat transfer, heat fluxes to the combustion chamber wall are highest during the combustion process and can reach as high as 10 MW/m^2 [35]. Reduction of the energy losses during these periods will result in an improvement of the engine efficiency.

The energy losses resulting from the transfer of heat to the cylinder walls is mainly through the piston crown, cylinder liner, combustion chamber, and valves. A decrease in the surface temperature of these components will lead to a reduction of the transfer of heat to the engine coolant and thus reduce energy losses. Figure 8 illustrates the main components in the energy loss process of the ICE.

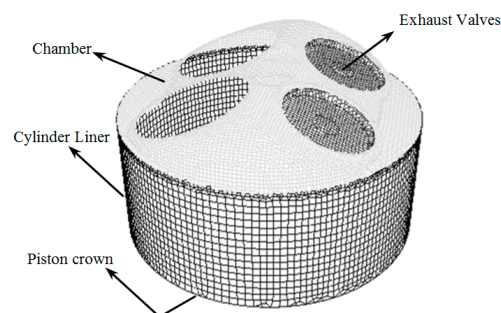


Figure 8. The main components involved in the energy loss process.

During the operation of an engine, heat is transferred by the motion of fluids and the relative motion between fluids and solid surfaces. During the latter stages of the compression stroke, combustion-expansion, and exhaust stroke, heat is transferred by convection between the in-cylinder gases, cylinder head, valves, and the cylinder wall.

In steady-flow convective heat transfer, the heat flux \dot{q} is expressed by the relation:

$$\dot{q} = h_c (T - T_W)$$

where h_c is the heat-transfer coefficient, T the temperature of flowing fluid stream, and T_W represents the temperature of the solid surface.

The heat absorption of water to form steam leads to the decrease in the average temperature of the working fluid in the cylinder (Figure 5). Through convectational heat transfer, the decrease in temperature T_W for the piston crown, cylinder liner, and combustion chamber among others are illustrated in Figures 9–12.

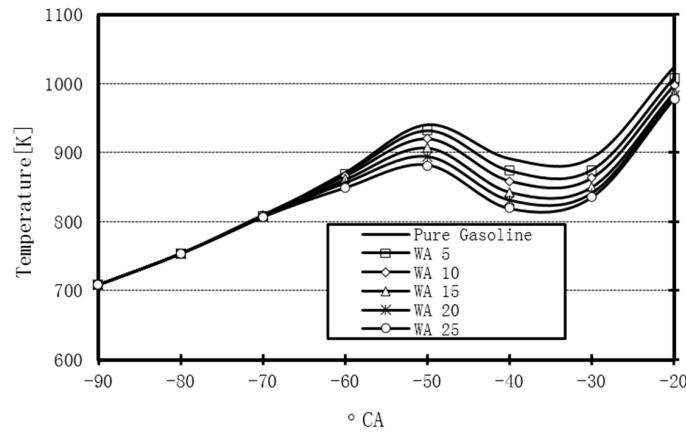


Figure 9. The decrease in average surface temperature T_W for the piston crown.

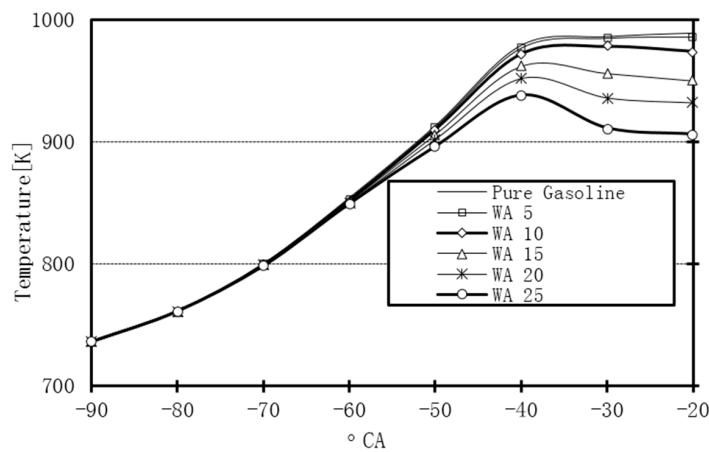


Figure 10. The decrease in average surface temperature T_W for the cylinder liner.

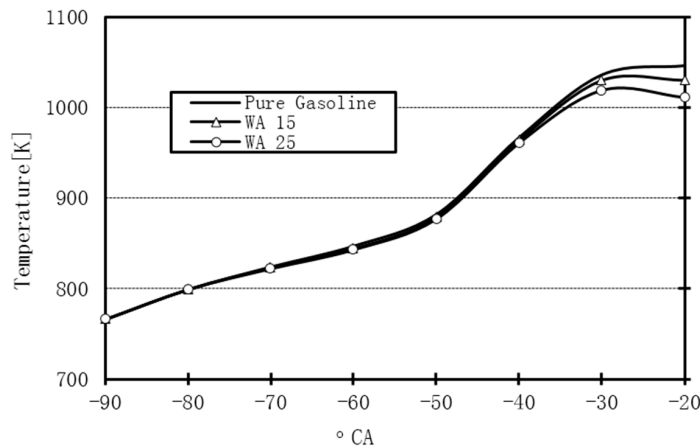


Figure 11. The decrease in average surface temperature T_W for the combustion chamber.

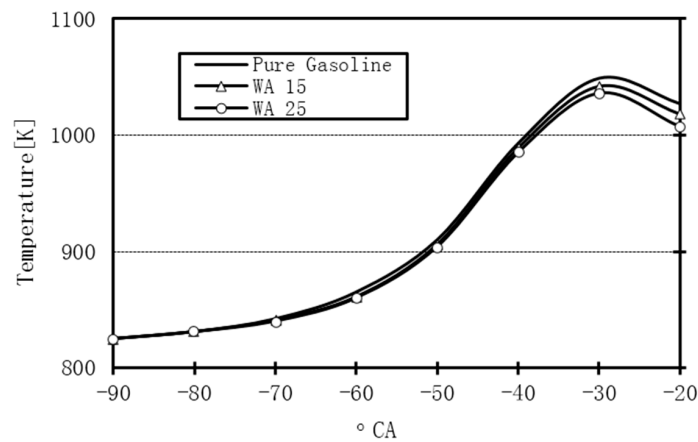


Figure 12. The decrease in average surface temperature T_W for the exhaust valves.

For Figures 9–12, as the WI mass into the cylinder increases, the average surface temperature T_W of the piston crown, cylinder liner, combustion chamber, and exhaust valves decreases. For 25% WI relative to the metered fuel mass and at 20° CA bTDC of ignition timing, the values of the decreasing average surface temperature were 46 K, 83 K, 35 K, and 20 K for the piston crown, cylinder liner, chamber, and exhaust valves, respectively. The decrease in the average surface temperature T_W of the piston crown and cylinder liner occurs earlier and is lower than that of the combustion chamber and exhaust valves because of the direction of the injected water, which is directed toward the piston head as indicated in Figure 13.

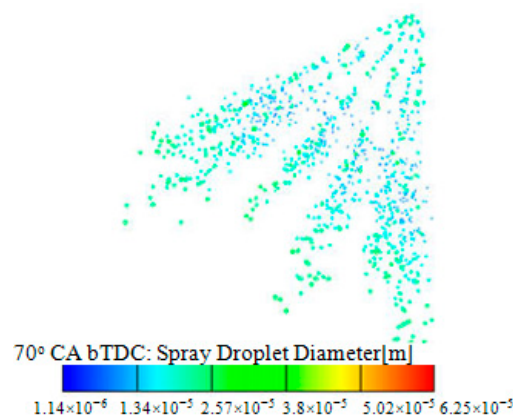


Figure 13. The water spray as directed towards the piston crown.

For the average surface temperature T_W of the piston crown and cylinder liner, the quick decrease in the temperature value was realized at 40° CA bTDC, and was earlier than that of the combustion chamber and exhaust valves. This is because the fuel sprayed impinges the piston crown and the cylinder liner. Figure 14 illustrates the fuel spray cloud at 40° CA bTDC.

The decrease of the average surface temperature T_W of the piston crown, cylinder liner, combustion chamber, and exhaust valves leads to a reduction in the conductive heat transfer in solids and heat losses to the engine coolant. The decrease in the average surface temperature of the cylinder liner also helps to prevent the deterioration of the lubricating oil film. Moreover, a lower average surface temperature of the cylinder walls has a significant positive effect on the avoidance of knock and pre-ignition problems which result from overheated hotspots in areas such as the piston crown, exhaust valves, combustion chamber, and spark plug electrodes.

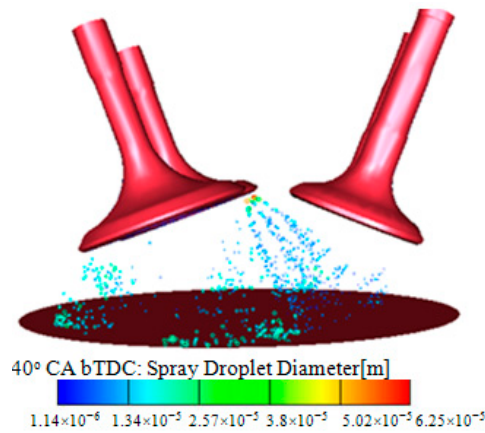


Figure 14. Amount of fuel spray impinging the piston crown and the cylinder liner.

3.1.3. Effects of Water Injection on Combustion

Employing WI during the compression stroke affects the combustion process because the heat absorption of the injected water results in the decrease of the in-cylinder pressure and working fluid temperature. The burning conditions are changed with the presence of injected water.

The effect of WI on the combustion process was evident by the fact that the burning time for the air-fuel mixture was extended. The injected water led to a decrease in the burning rate and the maximum brake torque was achieved by the use of WA [36].

Figure 15 illustrates the maximum temperature point for 15% WA in comparison with pure gasoline. For 15% WA, the maximum temperature point moved around 3–5° CA in comparison with of the use of pure gasoline with the point B occurring after TDC (after 0° CA).

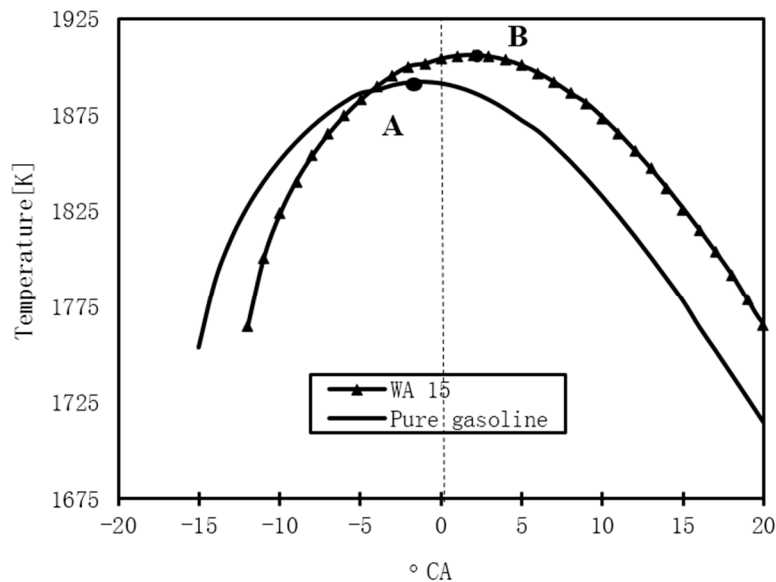


Figure 15. Effect of WI on the maximum temperature point.

3.1.4. Effect of WI on NO Emission

A major benefit of using WI in an engine is the reduction of NO emissions. In this study, the reduction of NO emissions was also achieved for WI during the compression stroke and is illustrated in Figure 16.

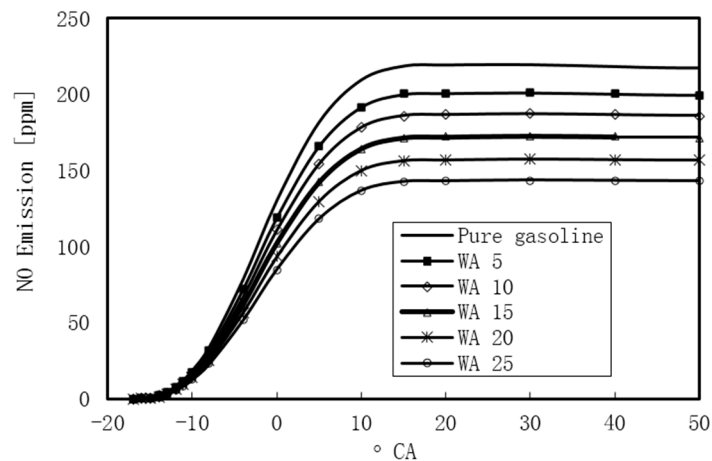


Figure 16. Effect of WI on reduction of the NO emission mass.

As the WI mass supplied to the engine increased, the NO emission mass decreased. For 25% of WA relative to the gasoline mass, the reduction of NO emission mass was 34%. For the highest peak-pressure case of 15% WA, the reduction of NO emission was about 21%. The main reason for realizing a reduction in NO emissions could be attributed to the fact that the injected water absorbed the heat of the compressed gases leading to reduced combustion temperatures. Figure 17 illustrates the contours for a high temperature region in the combustion chamber for 730° CA and 15% WA compared with the use of pure gasoline. C and C' denote high temperature areas of more than 2200 K for pure gasoline and 15% WA. The C' area is smaller than the area marked C and thus implies that the 15% WA case had a lower NO reaction rate than that of the pure gasoline case.

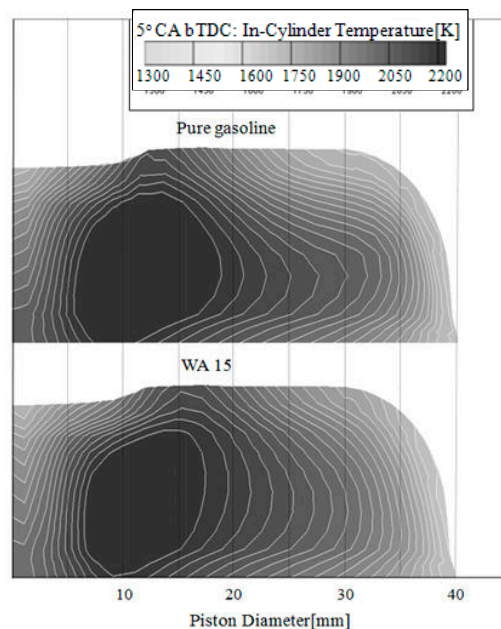


Figure 17. High temperature region in the combustion chamber at 5° CA bTDC.

WI leads to the reduction in the local temperature of the combustion regions within the cylinder. However, the maximum temperature of the working gasses in the cylinder for the WA cases was higher than that for the use of pure gasoline. Figure 18 presents the maximum temperature values for the various WA rates and the use of pure gasoline. 15% of WA gave the highest peak-pressure and the highest average temperature.

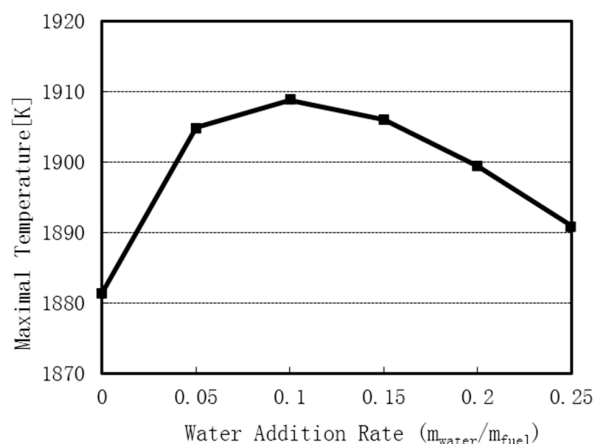


Figure 18. Maximal temperature values with various WA rates and the use of pure gasoline.

The effect of WA on charge gas was a decrease of the average temperature (Figures 4 and 5). The latent heat required to convert the injected water to vapor is absorbed from charge gases' energy. In the combustion process, the resulting steam increases the in-cylinder pressure in comparison to the pure gasoline (Figure 6). The effect of water injection on the decrease of in-cylinder temperature has been studied by many researchers [4,5,31]. Figure 18 presents maximal temperature values with various WA rates and pure gasoline. It is possible to notice that for a short period of time close to 0° CA, the maximum temperature in the chamber was higher in the WA case than in the pure gasoline case. The higher temperature for the WA case was due to a longer ignition delay period. The injected gasoline fuel had more time to mix with the surrounding hot gases, leading to higher pressure and heat released during the premixed combustion portion of the process. Therefore, a locally higher temperature was found. However, the effect of water injection on exhaust gas was a decrease of the in-cylinder temperature in relation to the use of pure gasoline, and is presented in the Section 3.2.3 of this study.

3.1.5. Effect of Water Temperature on the In-Cylinder Pressure

In this section, the effect of the injected water temperature on the in-cylinder pressure during the compression and combustion-expansion strokes is discussed. 15% of WA and various water temperatures varying between 40°C and 80°C were used to study the effect of water temperature on the in-cylinder pressure. The temperature factor did not show any significant effect on the compression pressure, as illustrated in Figure 19. The curve of compression pressure for various water temperatures was virtually the same.

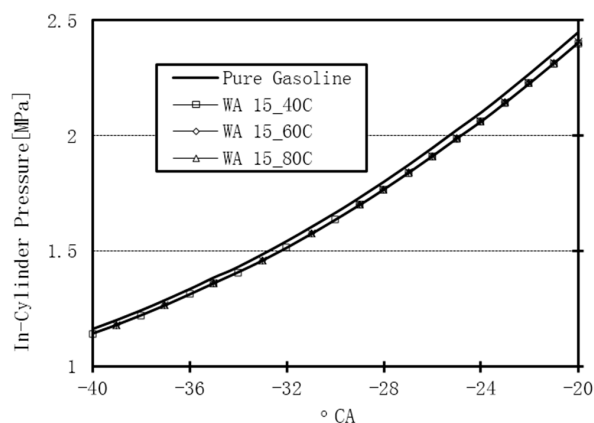


Figure 19. The effect of WI temperature on compression pressure.

However, during the combustion phase the WI temperature had an effect on the peak-pressure, as shown in Figure 20. The higher water temperature resulted in a higher peak pressure and thus a higher power output. The higher water temperature resulted in less heat being absorbed from the compressed gases and increased the peak pressure once there was volumetric expansion.

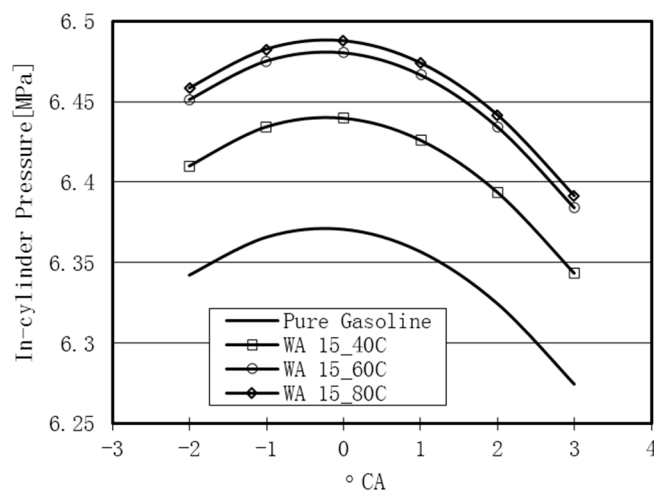


Figure 20. The effect of WI temperature on the peak-pressure.

WI had some effects on the in-cylinder pressure as a result of the heat absorption and the steam formation. The possible reduction in energy losses during the compression stroke, NO emission levels, and prolonged combustion were investigated for the various cases of WI. More WA mass (25%) helped to reduce the energy losses and NO emissions, but lowered the peak-pressure in comparison with the use of 15% WA mass.

3.2. Water Addition During the Expansion Stroke

Water can be injected into the cylinder during the expansion stroke to facilitate higher expansion pressure. The heat absorption from the high temperature of the burnt gases facilitated the volumetric expansion of steam, leading to an improvement in the work output. The WA mass rates used during the expansion stroke, among other details, are given in Table 4.

Table 4. WI parameters during the expansion stroke.

Item	Value
Injection Timing (° CA)	730
Water duration (° CA)	10
Water temperature [K]	373
Water mass [Kg]	100% (WA 1.0); 200% (WA 2.0); 300% (WA 3.0); 400% (WA 4.0) relative to fuel mass

3.2.1. Evaporation of Injected Water in the Cylinder

The liquid WI mass into the cylinder depended on the intake air mass, the temperature of compressed air, the water temperature, and the engine speed, among other parameters. The injection of excessive amounts of liquid water into the cylinder could result in poor evaporation and could have an effect on the corrosion resistance of the engine leading to a poor compatibility with the lubricating oil. Figure 21 presents the evaporation of injected water for the various WI masses at a water temperature of 100 °C.

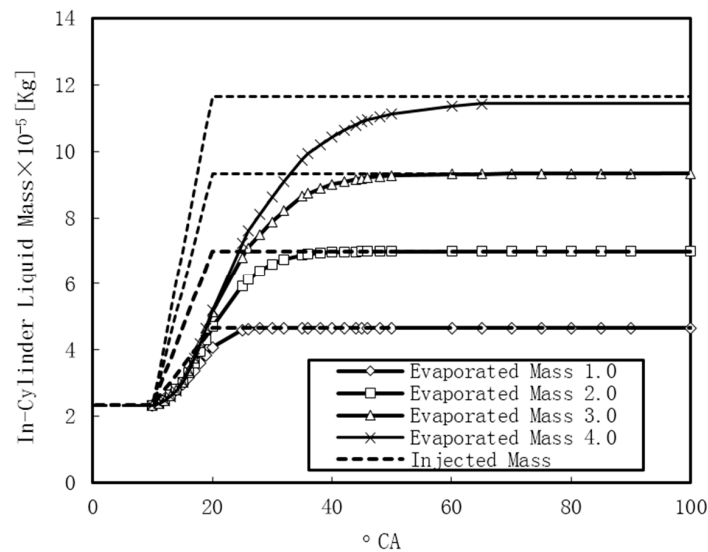


Figure 21. Relationship between the injected water mass and the evaporated water mass at 100 °C.

For a lower WA rate of 3.0, the total injected water mass was vaporized under the high temperature of the burning gases. A water injection rate of 4.0 WA by mass was not suitable for the current engine model because of its poor evaporation characteristics. Based on the relationship between the injected water mass and the vaporized mass, the water evaporation was not instantaneous, as illustrated in Figure 21. Increasing the WI mass increased the time required for complete evaporation. The time required for a complete evaporation of injected water at 25, 38, and 50° CA aTDC is shown in Figure 21 for the WA 1.0, WA 2.0, and WA 3.0 cases, respectively.

3.2.2. Effect of WI on Expansion Pressure

WI resulted in the decrease of the in-cylinder pressure in the first instance by heat absorption and a subsequent increase of the in-cylinder pressure via volumetric expansion in the second instance. Thus, the effect of injected water on the in-cylinder pressure was divided into two stages of pressure change in comparison with the pure gasoline case. During the first stage of WA, the in-cylinder pressure was lower than that of the use of pure gasoline with the opposite effect taking place in the second stage. Figure 22 illustrates the change of the in-cylinder pressure for WA 3.0 compared with the use of pure gasoline.

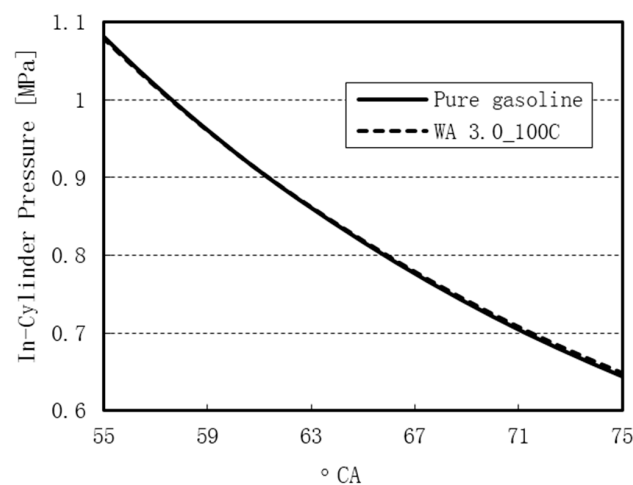


Figure 22. The variation of the in-cylinder pressure for WA 3.0 and pure gasoline.

Equation (1) gives an expression for the percentage increase of the in-cylinder pressure with the use of WI at 10° CA aTDC during the expansion stroke.

$$\text{Percentage [\%]} = \frac{[p_w - p_{pure}]}{p_{pure}} \times 100 \quad (1)$$

where p_w represents the in-cylinder pressure in the WI case with p_{pure} representing the in-cylinder pressure for pure gasoline.

As the WA mass increased, there was a decrease in the in-cylinder pressure during the first stage. For WA 3.0, the percentage decrease of the in-cylinder pressure was 2.7%. During the second stage, the injected water vaporized and expanded in volume. The percentage increase in the in-cylinder pressure was positive during this period. In Figure 23, the area of the positive percentage increase in the in-cylinder pressure was larger than the area of the percentage decrease in the in-cylinder pressure. Thus, the effect of WI on improving the power output can be achieved by the increase of the expansion pressure during the power stroke.

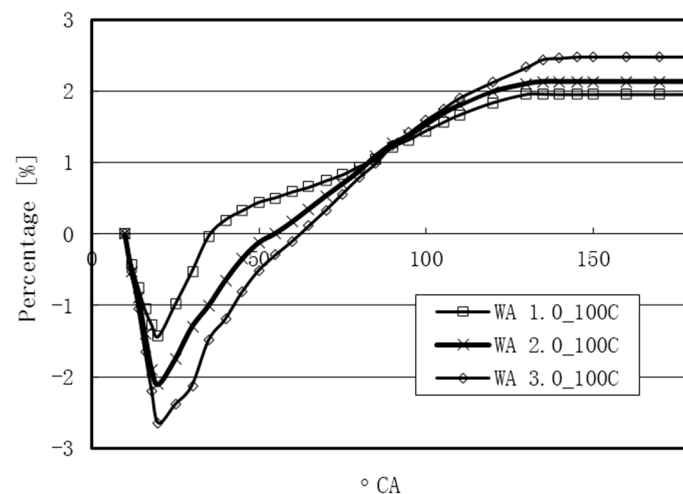


Figure 23. The percentage increase of the in-cylinder pressure.

3.2.3. Effect of WI on the Reduction in Energy Losses through In-Cylinder Heat Transfer to the Exhaust Gases

As mentioned earlier, 30%–40% of fuel energy is lost to exhaust gases. The rapid expansion of the burnt charge inside the cylinder produces turbulent fluid motions, high temperature regions, and large heat transfers from the fluid to the piston crown, cylinder wall, and combustion chamber. The rapid succession of working cycles in the cylinder creates an expanding exhaust gas with high pressure and temperature, which are scavenged from the cylinder in preparation for the next cycle while the exhaust gas is still expanding. The exhaust gas temperature is higher than that of ambient and contains thermal energy which is finally lost to the environment. Injection of liquid water will convert a portion of the heated gases produced from the combustion process energy into pressure, leading to an increase in the useful work. The decreasing temperature at the end of the expansion process will conduct heat, leading to a decrease in the exhaust gas temperature and therefore a reduced magnitude of wasted heat to the exhaust gases, as illustrated in Figure 24. At 180° CA aTDC, the exhaust gas temperature decrease was 42 K, 89 K, and 136 K for WA 1.0, WA 2.0, and WA 3.0 at 100 °C water temperature, respectively. Figure 25 presents the decreasing exhaust temperature with various water addition ratios in relation to the intake mass at the beginning of the exhaust process, in comparison with another study [25].

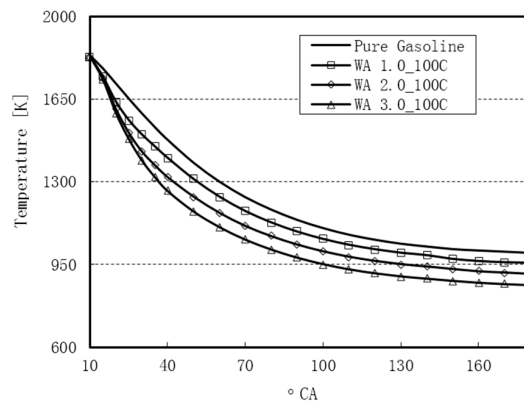


Figure 24. Decrease in exhaust gas temperature by the deployment of WI.

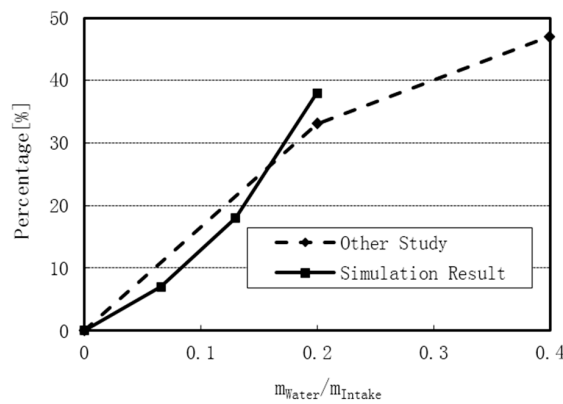


Figure 25. Percentage of decreasing exhaust gas temperature under various water addition ratios.

Moreover, the lower temperature of the expanding gases for WI in comparison with the pure gasoline case showed a decrease in the heat transfer to the cylinder walls in the process. According to Heywood [34], for a Diesel engine with a 45% indicated efficiency, 25% of the fuel energy is lost to the coolant in the cooling system. Of this 25%, 9% is lost during the exhaust stroke, 8% during the combustion stroke, 6% during the expansion stroke, and 2% due to friction. Reducing the surface temperature of the piston crown, cylinder liner, and combustion chamber will reduce the heat losses and improve the engine efficiency. Figures 26 and 27 illustrate the reduction of the surface temperature of the piston crown and combustion chamber during the expansion stroke for WA compared with the use of pure gasoline.

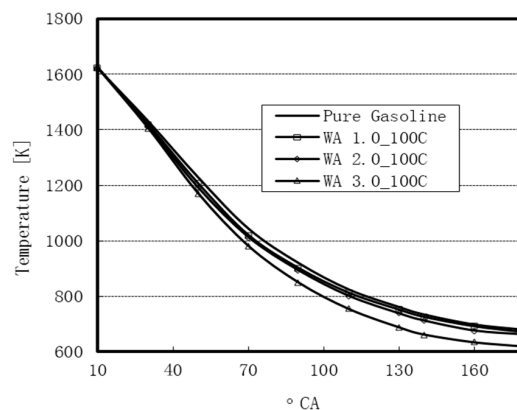


Figure 26. Decrease in the combustion chamber average temperature during the expansion process.

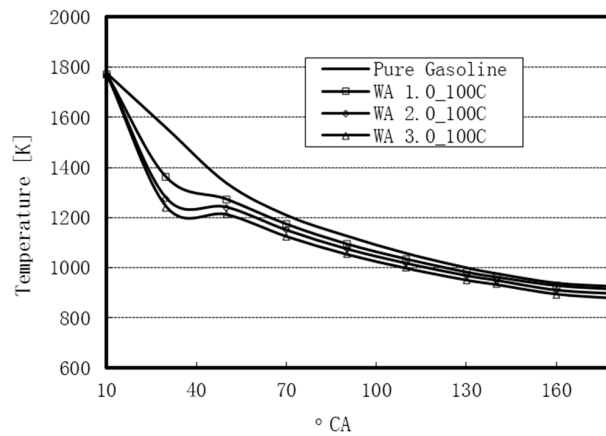


Figure 27. Decrease in the piston crown average temperature during the expansion process.

The effect of WI temperature on the percentage increase of the in-cylinder pressure is given in Figure 28. The water temperature was raised to 200 °C for direct injection into the cylinder. A water temperature of 200 °C was achieved by using the heat from the cooling system to heat the injected water in the first instance and the heat of the exhaust gases in the second instance. The water temperature had a positive and significant effect on the increase of the in-cylinder pressure. As the water temperature increased, the percentage decrease in pressure was lower. More than 4% of the increased pressure was realized during the second stage, where the volumetric expansion of steam for using a WA of 3.0 at a temperature of 200 °C took place. On the other hand, the percentage decrease in pressure during the first stage was only 1%.

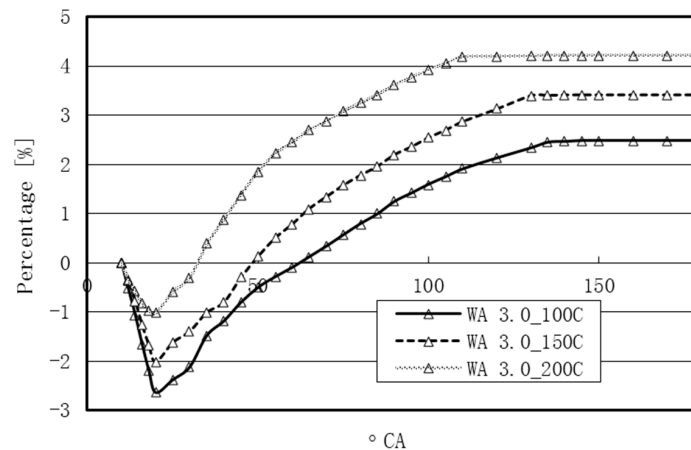


Figure 28. The effect of water temperature on the percentage increase of the in-cylinder pressure.

WI also showed a potential benefit of improved engine efficiency via waste heat recovery from the large amount of energy from the stream of exhaust gases.

3.3. Water Addition in Both Compression and Expansion Strokes

WI during the compression stroke had the benefits of reducing compression work and NO emission, and increasing the peak-pressure. Employing WI during the expansion stroke affected the expansion pressure in two stages: a decrease in pressure in the first stage of heat absorption and an increase in pressure at the second stage for the volumetric expansion of the steam formed. The useful advantages of WI cases can therefore be harnessed by using a sequence of timed WI during an engine cycle. For example, WI takes place for the first time during the compression stroke at 80° CA

bTDC with the second injection of water taking place during the expansion stroke at 10° CA aTDC. The parameters of WI in this section are presented in Table 5.

Table 5. WI parameters during the compression and expansion strokes.

Item	Value
1st WI	
Injection Timing	80° CA bTDC
Water duration [° CA]	10
Water temperature [K]	310
Water mass [Kg]	WA 15
2nd WI	
Injection Timing	10° CA aTDC
Water duration [° CA]	10
Water temperature [K]	200
Water mass [Kg]	3.0 WA

In this example, there was no percentage decrease in pressure because of the improved effect of the first WI on the in-cylinder pressure. In an internal combustion engine, as the expansion pressure increases, the work produced is higher. Figure 29 illustrates the time periods for the percentage increase in the in-cylinder pressure by using two water injections.

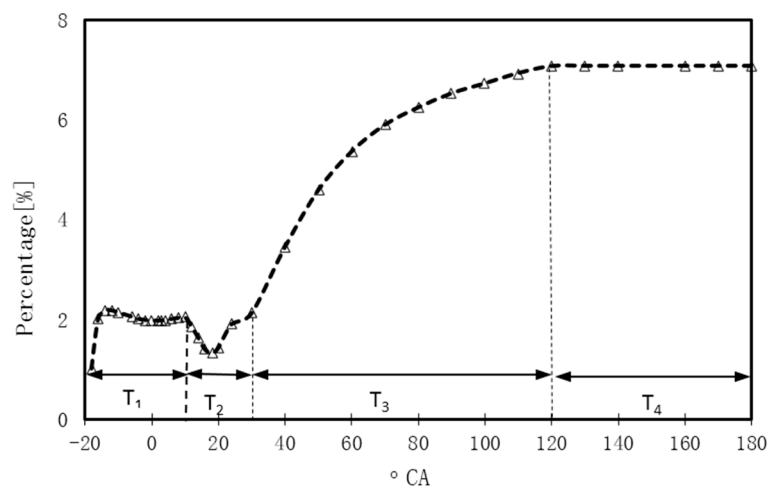


Figure 29. The percentage increase in the in-cylinder pressure during the two WI stages.

T₁: the percentage increase in the in-cylinder pressure because of the first WI.

T₂: the period for the second WI and its effect on the in-cylinder pressure due to heat absorption.

T₃: the percentage increase in the in-cylinder pressure because of evaporation during the second WI.

T₄: the percentage increase in the in-cylinder pressure due to the combined effect of the two water injections.

In this study, two temperatures of injected water were used to demonstrate the combined benefits of two WI timings described in Sections 3.1 and 3.2. The maximal percentage increase in pressure was around 7% with no decrease in the in-cylinder pressure during the expansion stroke. The same injected water temperature can be used to increase the expansion pressure, leading to a reduction in NO emissions.

On the whole, injected water presented opportunities for reducing NO emissions and for improving engine efficiency due to a reduction in heat losses. The heat absorption of injected water led to a decrease in the local temperature of the combustion areas and could decrease NO emissions.

The phase change process from liquid to gas increased the expansion pressure and improved the engine power output. The decrease in the average surface temperature of the cylinder liner and other hotspots helped to prevent deterioration of the lubricating oil film. This also enhanced the anti-knock resistance, and prolonged the engine lifespan. However, excessive water injection by mass could negatively affect the engine, in terms of ignition delay and cylinder corrosion. The disadvantages of the liquid WI method in ICEs need to be evaluated in detail before it is applied.

4. Conclusions

The results of a CFD simulation were carried out to investigate the effect of WA on the in-cylinder pressure and facilitate higher power output. Different timings of WI were used in this study and the following conclusions were drawn:

- (1) WI in the compression stroke facilitated a reduction in compression work, a 34% reduction in NO emission for the WA 25 case, and an increase in the peak pressure by a margin of about 2% for WA 15.
- (2) Employing WI during the expansion stroke indicated two stages of in-cylinder pressure change. For WA 3.0 and a water temperature of 100 °C, the percentage decrease in the in-cylinder pressure was 2.7% during the first stage with a percentage increase of about 2.5% during the second stage. WI helped to reduce the energy losses via heat transfer to the cylinder walls and the exhaust gases. At 180° CA aTDC, the exhaust gas temperature decreased by 42 K, 89 K, and 136 K for WA 1.0, WA 2.0, and WA 3.0, respectively. Increasing the WI temperature to 200 °C, the percentage decrease in the in-cylinder pressure was 1.0% during the first stage and more than 4.0% in the second stage.
- (3) Two timed water injections could be used to decrease the compression work and increase the pressure of the expanding burnt gases during the expansion stroke. The maximum percentage increase of the in-cylinder pressure was about 7% which showed the potential for achieving higher engine power output.

Acknowledgments: The authors would like to express their gratitude to the China Scholarship Council for providing financial support for this study in the form of CSC grant numbers 2012704029 and 2013GXZ993. The authors also wish to thank the National Research Project Fund, China (Grant Number 51276132) for additional financial support for this study. The input of various anonymous reviewers regarding how the original manuscript could be improved was greatly appreciated.

Author Contributions: This is to confirm that all authors have contributed in diverse ways from the design of the research to the final manuscript preparation.

Conflicts of Interest: The authors declare no potential conflicts of interest.

References

1. Nande, A.M.; Wallner, T.; Naber, J. Influence of water injection on performance and emissions of a direct-injection hydrogen research engine. *SAE Int.* **2008**. [[CrossRef](#)]
2. Gadallah, A.H.; Elshenawy, E.A.; Elzahaby, A.M.; El-Salmawy, H.A.; Bawady, A.H. Effect of in cylinder water injection strategies on performance and emissions of a hydrogen fuelled direct injection engine. *SAE Int.* **2009**. [[CrossRef](#)]
3. Özcan, H.; Söylemez, M. Thermal balance of a lpg fuelled, four stroke si engine with water addition. *Energy Convers. Manag.* **2006**, *47*, 570–581. [[CrossRef](#)]
4. Lanzafame, R. Water Injection Effects in a Single-cylinder CFR Engine. *SAE Int.* **1999**. [[CrossRef](#)]
5. Tauzia, X.; Maiboom, A.; Shah, S.R. Experimental study of inlet manifold water injection on combustion and emissions of an automotive direct injection diesel engine. *Energy* **2010**, *35*, 3628–3639. [[CrossRef](#)]
6. Karagöz, Y.; Yüksek, L.; Sandalcı, T.; Dalkılıç, A. An experimental investigation on the performance characteristics of a hydroxygen enriched gasoline engine with water injection. *Int. J. Hydrog. Energy* **2015**, *40*, 692–702. [[CrossRef](#)]

7. Feng, R.; Yang, J.; Zhang, D.; Deng, B.; Fu, J.; Liu, J.; Liu, X. Experimental study on si engine fuelled with butanol–gasoline blend and h₂o addition. *Energy Convers. Manag.* **2013**, *74*, 192–200. [[CrossRef](#)]
8. Munsin, R.; Laonual, Y.; Jugjai, S.; Imai, Y. An experimental study on performance and emissions of a small si engine generator set fuelled by hydrous ethanol with high water contents up to 40%. *Fuel* **2013**, *106*, 586–592. [[CrossRef](#)]
9. Sari, R.L.; Tatsch, G.A.; Dalla Nora, M.; dos Santos Martins, M.E.; LanzaNova, T.D.M. Combustion performance of high water content hydrous ethanol. In Proceedings of the Virtual Powertrain Conference, São Paulo, Brasil, 22–23 August 2013.
10. Boretti, A.; Osman, A.; Aris, I. Direct injection of hydrogen, oxygen and water in a novel two stroke engine. *Int. J. Hydrog. Energy* **2011**, *36*, 10100–10106. [[CrossRef](#)]
11. Liu, J.; Fu, J.; Feng, K.; Wang, S.; Zhao, Z. Characteristics of engine exhaust gas energy flow. *J. Cent. South Univ. Sci. Technol.* **2011**, *42*, 3370–3376.
12. Stabler, F. Automotive Applications of High Efficiency Thermoelectrics. In Proceedings of the DARPA/ONR/DOE High Efficiency Thermoelectric Workshop, San Diego, CA, USA, 24–27 March 2002; pp. 1–26.
13. Taylor, C. Automobile engine tribology—Design considerations for efficiency and durability. *Wear* **1998**, *221*, 1–8. [[CrossRef](#)]
14. Anderson, B.S. Company perspectives in vehicle tribology-volvo. *Tribol. Ser.* **1991**, *18*, 503–506.
15. Mahlia, T.; Saidur, R.; Memon, L.A.; Zulkifli, N.; Masjuki, H. A review on fuel economy standard for motor vehicles with the implementation possibilities in malaysia. *Renew. Sustain. Energy Rev.* **2010**, *14*, 3092–3099. [[CrossRef](#)]
16. Priest, M.; Taylor, C. Automobile engine tribology—Approaching the surface. *Wear* **2000**, *241*, 193–203. [[CrossRef](#)]
17. Wang, E.; Zhang, H.; Zhao, Y.; Fan, B.; Wu, Y.; Mu, Q. Performance analysis of a novel system combining a dual loop organic rankine cycle (orc) with a gasoline engine. *Energy* **2012**, *43*, 385–395. [[CrossRef](#)]
18. Dolz, V.; Novella, R.; García, A.; Sánchez, J. Hd diesel engine equipped with a bottoming rankine cycle as a waste heat recovery system. Part 1: Study and analysis of the waste heat energy. *Appl. Therm. Eng.* **2012**, *36*, 269–278. [[CrossRef](#)]
19. Wang, Y.; Dai, C.; Wang, S. Theoretical analysis of a thermoelectric generator using exhaust gas of vehicles as heat source. *Appl. Energy* **2013**, *112*, 1171–1180. [[CrossRef](#)]
20. Gewald, D.; Karellas, S.; Schuster, A.; Spliethoff, H. Integrated system approach for increase of engine combined cycle efficiency. *Energy Convers. Manag.* **2012**, *60*, 36–44. [[CrossRef](#)]
21. Hatazawa, M.; Sugita, H.; Ogawa, T.; Seo, Y. Performance of a thermoacoustic sound wave generator driven with waste heat of automobile gasoline engine. *Nippon Kikai Gakkai Ronbunshu B Hen (Trans. Jpn. Soc. Mech. Eng. Part B)* **2004**, *16*, 292–299. (In Japanese) [[CrossRef](#)]
22. Yu, C.; Chau, K. Thermoelectric automotive waste heat energy recovery using maximum power point tracking. *Energy Convers. Manag.* **2009**, *50*, 1506–1512. [[CrossRef](#)]
23. Yang, J. Potential Applications of Thermoelectric Waste Heat Recovery in the Automotive Industry. In Proceedings of the 24th International Conference on Thermoelectrics, Clemson, SC, USA, 19–23 June 2005; pp. 170–174.
24. Vázquez, J.; Sanz-Bobi, M.A.; Palacios, R.; Arenas, A. State of the Art of Thermoelectric Generators Based on Heat Recovered from the Exhaust Gases of Automobiles. Available online: http://www.iit.comillas.edu/palacios/thermo/EWT02-Exhaust_gases.pdf (accessed on 19 September 2016).
25. Zhu, S.; Deng, K.; Qu, S. Thermodynamic analysis of an in-cylinder waste heat recovery system for internal combustion engines. *Energy* **2014**, *67*, 548–556. [[CrossRef](#)]
26. Fu, J.; Liu, J.; Ren, C.; Wang, L.; Deng, B.; Xu, Z. An open steam power cycle used for ic engine exhaust gas energy recovery. *Energy* **2012**, *44*, 544–554. [[CrossRef](#)]
27. Endo, T.; Kawajiri, S.; Kojima, Y.; Takahashi, K.; Baba, T.; Ibaraki, S.; Takahashi, T.; Shinohara, M. Study on Maximizing Exergy in Automotive Engines. *SAE Int.* **2007**. [[CrossRef](#)]
28. Bari, S.; Hossain, S.N. Waste heat recovery from a diesel engine using shell and tube heat exchanger. *Appl. Therm. Eng.* **2013**, *61*, 355–363. [[CrossRef](#)]
29. Sarabchi, N.; Saray, R.K.; Mahmoudi, S. Utilization of waste heat from a hcci (homogeneous charge compression ignition) engine in a tri-generation system. *Energy* **2013**, *55*, 965–976. [[CrossRef](#)]

30. Yamada, N.; Mohamad, M.N.A. Efficiency of hydrogen internal combustion engine combined with open steam rankine cycle recovering water and waste heat. *Int. J. Hydrog. Energy* **2010**, *35*, 1430–1442. [[CrossRef](#)]
31. Wu, Z.-J.; Yu, X.; Fu, L.-Z.; Deng, J.; Hu, Z.-J.; Li, L.-G. A high efficiency oxyfuel internal combustion engine cycle with water direct injection for waste heat recovery. *Energy* **2014**, *70*, 110–120. [[CrossRef](#)]
32. Kurniawan, W.H.; Abdullah, S. Numerical analysis of the combustion process in a four-stroke compressed natural gas engine with direct injection system. *J. Mech. Sci. Tech.* **2008**, *22*, 1937–1944. [[CrossRef](#)]
33. Abdullah, S.; Kurniawan, W.H.; Shamsudeen, A. Numerical analysis of a combustion process in a compressed natural gas direct injection engine. *J. Appl. Fluids Mech.* **2008**, *1*, 65–86.
34. El Tahry, S.H. K-epsilon equation for compressible reciprocating engine flows. *J. Energy* **1983**, *7*, 345–353. [[CrossRef](#)]
35. Heywood, J.B. *Internal Combustion Engine Fundamentals*; Mcgraw-hill: New York, NY, USA, 1988; Volume 930.
36. Harrington, J. Water Addition to Gasoline-Effect on Combustion, Emissions, Performance, and Knock. *SAE Int.* **1982**. [[CrossRef](#)]



© 2016 by the authors; licensee MDPI, Basel, Switzerland. This article is an open access article distributed under the terms and conditions of the Creative Commons Attribution (CC-BY) license (<http://creativecommons.org/licenses/by/4.0/>).